16th World Conference on Earthquake, 16WCEE 2017

Santiago Chile, January 9th to 13th 2017

Paper N° 2709

Registration Code: S-D1463099082

INTERMEDIATE-STORY COLLAPSE OF REINFORCED CONCRETE BUILDINGS CONSIDERING AFTERSHOCKS

T. Nakamura [1] and A. Kawami [2]

[1] *Associate Professor, Niigata University, takaya@eng.niigata-u.ac.jp*
[2] *Hokuriku Gas Co., Ltd.*

Abstract

This study focuses on the intermediate-story collapse that is often seen in old reinforced concrete (RC) buildings of around 10 stories with brittle columns. Once buildings are damaged by the main shock, it is important to evaluate the effect of aftershocks to judge whether to continue to use the damaged buildings. Thus, this study aims to examine the intermediate-story collapse of RC buildings, with consideration of aftershocks, by conducting dynamic analysis. Nine- and three-story buildings are analyzed. The buildings are represented by equivalent shear building models. Model lateral load versus inter-story drift relations are represented based on past collapse tests of brittle columns. Strength deterioration after maximum load is considered. Dynamic analysis is performed for various columns and ground motions, and responses of the model buildings in the post-peak regions, including collapse, are studied. Relations between the maximum drift in the main shock and the level of aftershock that induces collapse are discussed. The study reveals that the smaller the maximum drift in the main shock, the smaller the ground motion level of aftershocks that induce collapse for short-period ground motions. This result is different from the general perception. The finding shows that elongation of the period of buildings due to the large plastic response in the main shock induces the discrepancy between the period of buildings and that of ground motions of aftershocks.

Keywords: Reinforced concrete; Intermediate-story collapse; Shear failure; Aftershock

1. Introduction

Many reinforced concrete (RC) buildings with brittle columns are in danger of story collapse in the event of future earthquakes. This study focuses on the intermediate-story collapse, which has often been seen for around 10-story old buildings during past severe earthquakes such as the 1995 Kobe earthquake. The intermediate-story collapse occurrs due to shear failure and the following axial collapse of columns. Once buildings are damaged, it is important to evaluate the effect of aftershocks to judge whether to continue using the damaged buildings. While analytical researches of the effect of aftershocks for buildings have been undertaken [1, 2, 3, et al.], the evaluations considering intermediate-story collapse of buildings with column's shear failure are yet to be conducted. Thus, this study aims to examine the intermediate-story collapse of RC buildings, with consideration of aftershocks, by conducting dynamic analysis. Nine- and three-story buildings are analyzed, and responses of the model buildings in the post-peak regions, including collapse, are studied. Relations between the maximum drift in the main shock and the level of aftershock that induces collapse are discussed. In addition, the effects of a predominant period of ground motion (short-period or long-period) and the number of stories on the dynamic responses are assessed.

2. Outline of analysis

2.1 Analytical model

This study analyzes RC buildings designed according to pre-1971 Japanese building codes. In 1971, the regulations for transverse reinforcement ratios were strengthened. This study is based on buildings with nine and three stories. The main discussion is based on nine-story buildings. The steps in the analysis are outlined below.

(1) The buildings are represented by equivalent shear building models. They are designed to comprise a single column line and a rigid beam. Conventional member to member analysis cannot be used for this case because it is impossible at present to represent the column axial behavior at and after the collapse realistically. The analytical model of a nine-story building is shown in Fig. 1. The height and weight of each story are assumed to be 3600 mm and 753 kN, respectively. The structural properties of the nine-story building's analytical model are summarized in Table 1.

(2) Model building comprises a brittle column (clear height h_0 = 2400 mm, column section width b × depth D = 600 mm × 600 mm, and h_0/D = 4). Fig. 2 shows the idealized column, which is assumed to be twice as large as the tested specimens [4].

(3) Story strength distribution is determined based on uniform design load distribution prescribed by the old building code before 1971. However, according to the construction practice where the column size for the top two or three stories is constant, it is assumed that the all stories of the three-story building has the same strength, while the nine-story building has the same strength for the top three stories. It is also assumed that in previous earthquakes where only a single story collapsed and the damage to other stories was negligible, the collapsed story was weaker than the other stories. For analysis, the third story from the top is selected as the "collapse story" and its strength is reduced to 80% of the previously determined strength. Fig. 3 compares the story strength distribution of the analytical model and the lateral strength required by the old building code for a nine-story building. As a result, the model buildings are expected to collapse at the third story from the top. Although the three-story building does not collapse at an intermediate-story, it is used as a comparison to the intermediate-story collapses of nine-story buildings.

(4) The seismic capacity index I_S is computed for each story by using the second-level procedure from the Standard for Seismic Evaluation [5, 6]. The strength of each story is determined such that the value for I_S for the collapse story is 0.4. In Japan, the value of I_S is commonly used to evaluate the seismic performance of existing RC buildings. It is widely recognized that when $I_S \geq 0.6$, such buildings do not suffer severe damage or collapse even during severe earthquakes. Note that the I_S value for buildings designed under the old building code is generally 0.4 [7]. As described in the Appendix, the I_S value is calculated based on the product of the strength index C and the deformability index F. The index C is defined as the strength of a column divided by

the total weight of floors above the column, and the index F is determined based on the deformability of a column. The F values of columns that are twice the size of the tested samples are computed to be 1.0. Because of the assumed distribution of story strength, I_S takes on its lowest value at the collapse story. Hereinafter, I_S for the collapse story is considered to be applicable to the entire building.

(5) The initial distribution of story stiffness is the same as the distribution of story strength. The initial stiffness of each story is such that the first mode periods are 0.65 s and 0.22 s, respectively, for the nine- and three-story buildings, which are computed using the conventional equation $T = 0.02\ h$, where h is the total building height in meters.

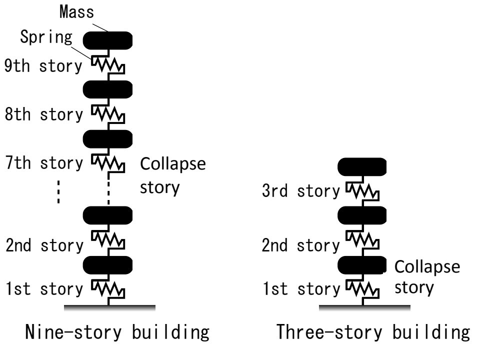

Fig. 1 – Analytical model

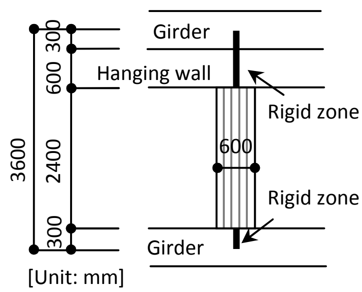

Fig. 2 – Idealized column

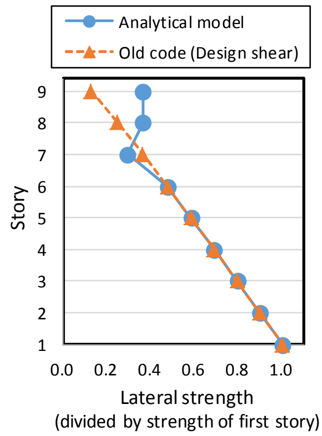

Fig. 3 – Story strength distribution (nine-story building)

Table 1 – Structural properties of the analytical model (nine-story building)

Story	Weight (kN)	Initial stiffness (kN/cm)	Strength (kN)	C	F	$1/Ai$	I_S
9	753	1510	1820	2.42	1.0	0.44	1.07
8	753	1510	1820	1.21	1.0	0.54	0.66
7	753	1210	1460	0.65	1.0	0.62	0.40
6	753	1930	2380	0.79	1.0	0.68	0.54
5	753	2300	2920	0.78	1.0	0.74	0.58
4	753	2630	3450	0.76	1.0	0.80	0.61
3	753	3070	3970	0.75	1.0	0.86	0.65
2	753	3510	4490	0.75	1.0	0.93	0.69
1	753	3950	5020	0.74	1.0	1.00	0.74

2.2 Hysteresis model

Model lateral load versus inter-story drift relations are represented by a quadrilinear function based on past collapse tests [4]. The specimens simulating brittle columns were tested under constant axial load (an axial stress ratio of 0.2) and loaded until they are unable to sustain the axial load. Three columns, labeled S1, S2, and FS1, are used for the model. The longitudinal bar ratios (p_g), defined as the total main reinforcement areas divided by the column section, are 2.65% for columns S1 and S2 and 1.69% for column FS1. The transverse bar ratios (p_w) are 0.21% for columns S1 and FS1 and 0.14% for column S2. Relations between the lateral load and inter-story drift of the test results and analytical models, and photos taken at collapse, are shown in Fig. 4. The inter-story drift angle is translated from the drift angle by applying the geometric shape shown in Fig. 2. Columns S1 and S2 fail in shear before flexural yielding and lost axial load-carrying capacity, or collapse at inter-story drift of 8.9% and 3.6%, respectively, whereas column FS1 fails in shear after flexural yielding and collapse at inter-story drift of 3.5%.

The Takeda-slip model [8] incorporating strength deterioration after maximum load is used in the dynamic analysis (Fig. 4). Lateral load versus inter-story drift relations are represented by a quadrilinear function. The frameworks prior to maximum loading are the same for the three columns. Loading at the first break point (crack point) is 33% of the maximum load. Inter-story drift at the maximum load is assumed to be uniform for all stories at 0.67%. Inter-story drift at the third break point is assumed to be uniform for all stories at 1.3%. Loading at the third break point of columns S1 and S2 is 50% of the maximum load, whereas that of column FS1 is 100% of the maximum load. As stated above, the collapse drifts for columns S1, S2, and FS1 are 8.9%, 3.6%, and 3.5%, respectively. Loading at the collapse point is assumed to be zero for columns S1 and S2 and 80% of the maximum load for column FS1. Note that S2 and FS1 have almost the same collapse drift and different types of strength deterioration. The collapse drift is set as uniform for all stories of the three-story building and the top three stories of the nine-story buildings. However, it is reduced proportionally under the third story from the top as the story decreases, taking into consideration the large axial load for these stories. Table 2 shows the collapse drifts of columns S1, S2, and FS1. In Table 2, underlines indicate the collapse story. Collapse drifts of the collapse stories of nine- and three-story buildings are the same because the axial load of the collapse stories are the same.

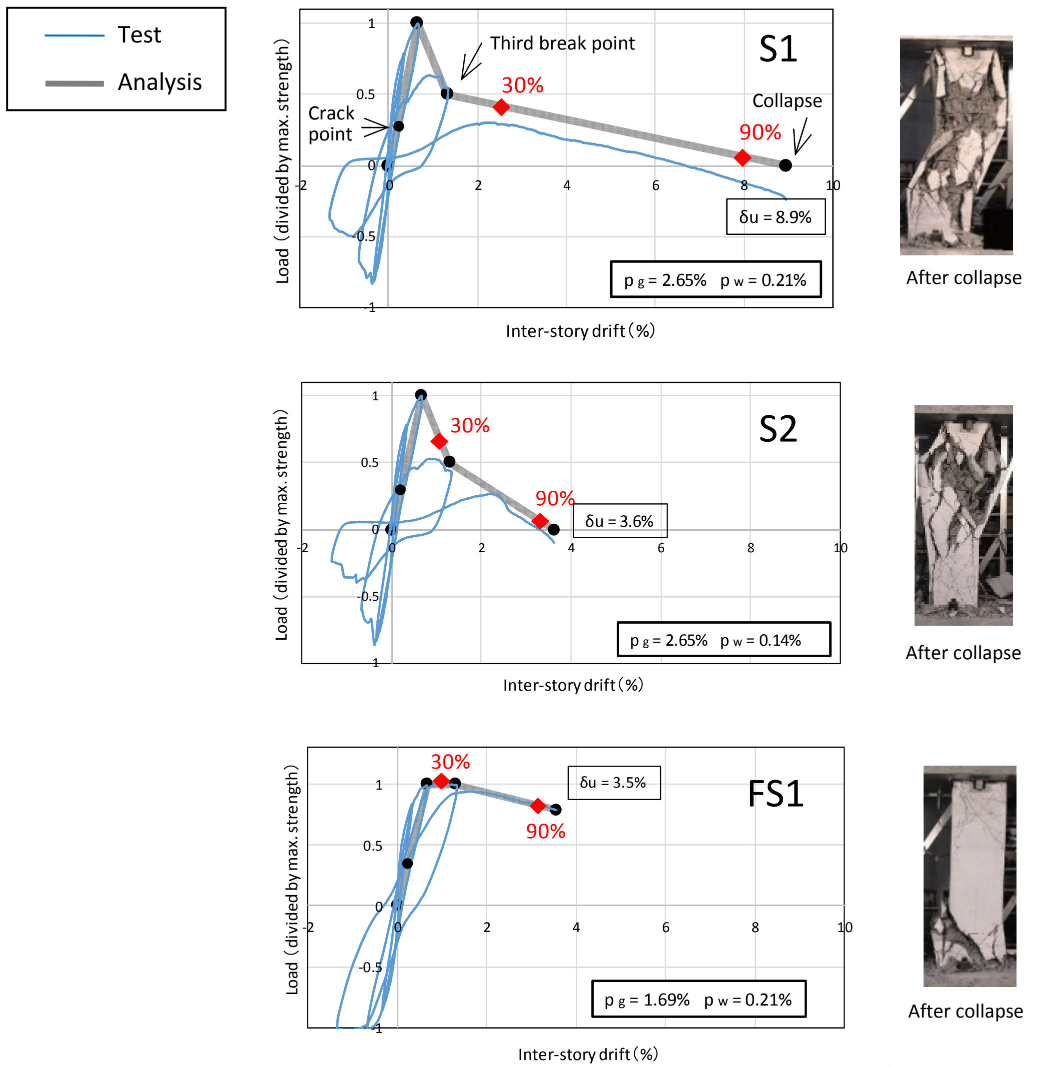

Fig. 4 – Load versus drift (collapse story) and damage condition

Table 2 – Collapse drift (columns S1, S2, and FS1)

(a) nine-story building

Story	S1	S2	FS1
9	8.9	3.6	3.5
8	8.9	3.6	3.5
7	8.9	3.6	3.5
6	8.5	3.2	3.3
5	8.0	3.2	3.2
4	7.6	3.1	3.0
3	7.1	2.9	2.8
2	6.7	2.7	2.6
1	6.3	2.5	2.5

(b) three-story building

Story	S1	S2	FS1
3	8.9	3.6	3.5
2	8.9	3.6	3.5
1	8.9	3.6	3.5

[%]

The framework of the hysteresis is based on the Takeda-slip model [8]. Fig. 5 compares lateral loading to inter-story drift of the test and the analytical model results for column S2. The test results in Fig. 5, indicate that, after the shear failure, the orientation after reversal of the load is not toward the preceding maximum deformation point, but toward the symmetrical point with respect to the origin of the load reversal point. To represent such hysteresis rules of RC columns with shear failure (columns S1 and S2), Takeda-slip model is modified to be consistent with the rule of the orientation (see Fig. 5, points A to B).

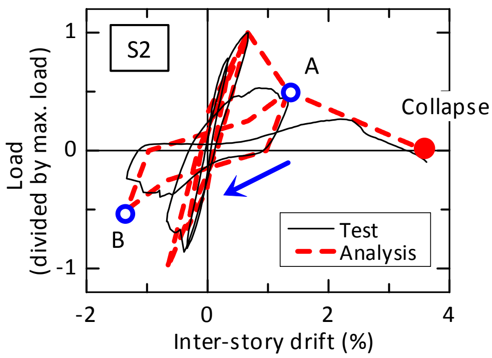

Fig. 5 – Rules for the hysteresis

2.3 Dynamic analysis

Viscous damping is proportional to initial stiffness because, if viscous damping proportional to instantaneous stiffness is used, acceleration (not damping) results in regions of negative instantaneous stiffness. The damping ratio is set at 1%. The numerical integration method is from Newmark's β method ($\beta = 0.25$) [9]. Because lateral loads measured in the test include the so-called P-Δ effect, this effect is not considered in the analysis.

2.4 Ground motion

Six ground motions recorded during previous severe earthquakes are used for the analysis (see Table 3; JMA at the 1995 Southern Hyogo Prefecture earthquake, ELC at the 1940 Imperial Valley earthquake, TOH at the 1978 Miyagiken-oki earthquake, MXC at the 1985 Mexico earthquake, TMK at the 2003 Tokachi-oki earthquake, and CYT at the 2011 off the Pacific coast of Tohoku earthquake). Table 3 shows the maximum ground velocities

V_{max} from the original level of ground motions. Note that V_{max} is calculated as the maximum response velocity for an elastic single-degree-of-freedom system with a natural period of 10 s and a damping ratio of 0.707% [10].

Upon conducting the analyses, the level of ground motion is adjusted based on the maximum ground velocity V_{max}. In Japan, such normalization based on V_{max} is commonly used to evaluate the seismic intensity of earthquake motions in buildings. Fig. 6 shows the spectrum of acceleration for earthquakes with V_{max} of 50 cm/s. In the figure, the damping ratio is 5%. According to Fig. 6, the response acceleration rises sharply around the natural period of 0.5 s for most ground motions. Note that earthquakes MXC and TMK have peaks of response acceleration at the natural periods of approximately 2 and 3 s, respectively. Earthquake CTY also has larger response accelerations with a natural period of approximately 2 s or more. Thus, in this study, earthquakes MXC, TMK, and CYT are deemed as long-period ground motions, whereas earthquakes JMA, ELC, and TOH are deemed as short-period ground motions.

The levels of main shocks are adjusted such that the maximum drift would be 30% or 90% of the collapse drift. Each point is shown in Fig. 4. Aftershocks (in the same way as the main shock) are input successively and the level is adjusted so that the buildings are collapsed to identify the level necessary to induce collapse. Thus, the relations between the maximum drift in the main shock and the smallest level of aftershock that induces collapse are discussed.

Table 3 – Ground motions (original level)

Name	Site, Direction	Year, Earthquake	Maximum ground velocity V_{max} (cm/s)	Short-period or long-period
JMA	Japan Meteorological Agency Kobe, NS	1995, Southern Hyogo Prefecture	82.6	Short period
ELC	El Centro, NS	1940, Imperial Valley	33.6	Short period
TOH	Tohoku University, NS	1978, Miyagiken-oki	41.6	Short period
MXC	SCT1, EW	1985, Mexico	60.6	Long-period
TMK	Japan Meteorological Agency Tomakomai, NS	2003, Tokachi-oki	16.3	Long-period
CYT	Japan Meteorological Agency Chiyoda-ku, EW	2011, off the Pacific coast of Tohoku	21.0	Long-period

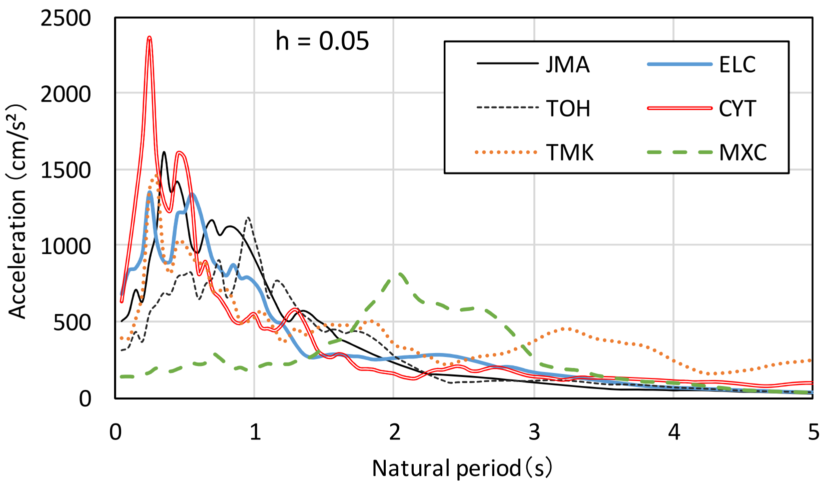

Fig. 6 – Acceleration spectrum (V_{max} = 50 cm/s)

3. Analytical results

Dynamic analysis is performed for the three columns and various ground motions. The calculations terminate when the response drift equals the collapse drift. The collapse story is computed to suffer the greatest damage in most cases; therefore, the analytical results for the collapse story are presented as follows.

3.1 Collapse procedure

As an example of the collapse procedure, Fig. 7(a) shows the time history of ground acceleration and inter-story drift and Fig. 7(b) shows the relation between lateral load and inter-story drift for the nine-story building with column S2 and the input motion of TMK. In the main shock, the maximum inter-story drift is 30% of the collapse drift when the maximum ground velocity V_{max} is 39.2 cm/s. In the aftershock, the inter-story drift increases and the building collapses when V_{max} is 39.0 cm/s. In this case, the smallest level of aftershock that induces collapse is almost the same as the main shock.

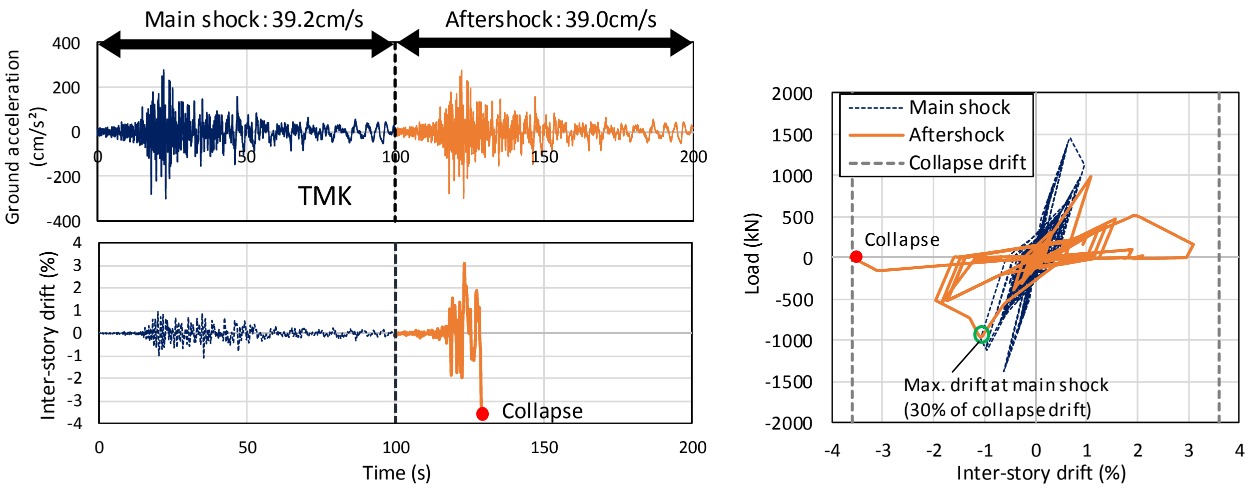

(a) Time histories of ground acceleration and drift (b) Load versus drift

Fig. 7 – Analytical results (nine-story building, column S2, TMK)

3.2 Relationship between ground-motion level of main shock and aftershock

Fig. 8 compares the ground motion level (maximum ground velocity) of the main shock and that of the aftershock for columns S1, S2, and FS1. In each figure, analytical results of the nine- and three-story buildings are shown altogether. In Fig. 8, the analytical results are shown separately by short- and long-period ground motions.

For column S1 (see Fig. 8(a)), the ground motion-levels of the aftershock are larger than those of the main shock for short-period ground motions (JMA, ELC, and TOH). In contrast, the ground motion levels of the aftershock are smaller than those of the main shock for long-period ground motions (MXC, TMK, and CYT). The reason is explained as follows. A plastic response causes elongation of the natural period, and the degree of such period elongation of buildings increases with the collapse drift. Thus, column S1 with its large collapse drift has a long natural period of the building after the main shock and tends to resonate with the aftershock of long-period input motion, but resonates only slightly with short-period input motion. This result indicates that if a building with a large collapse drift experiences a large response drift and suffers severe damage in the main shock, long-period ground motions are more dangerous for it than short-period ground motions.

For columns S2 and FS1 (see Fig. 8(b) and (c)), the ground motion-levels of the aftershock are almost the same as those of the main shock for short-period ground motions. This is because columns S2 and FS1 have smaller collapse drifts than S1 and collapse easily with smaller aftershock ground motion levels. For long-period ground motions, columns S2 and FS1 exhibits the same tendency as column S1.

For long-period ground motions, trends polarize into two groups. Maximum ground velocities in the main shock for MXC are larger than those for CYT and TMK. This is because MXC includes few short-period components (see Fig. 6). Thus, large maximum ground velocities in the main shock are required to obtain the target inter-story drifts.

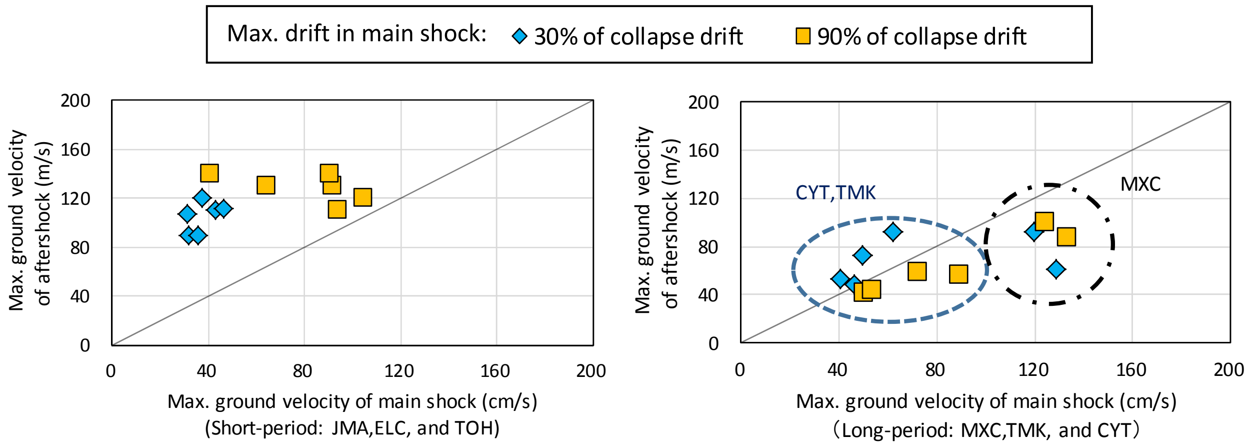

(a) Model S1

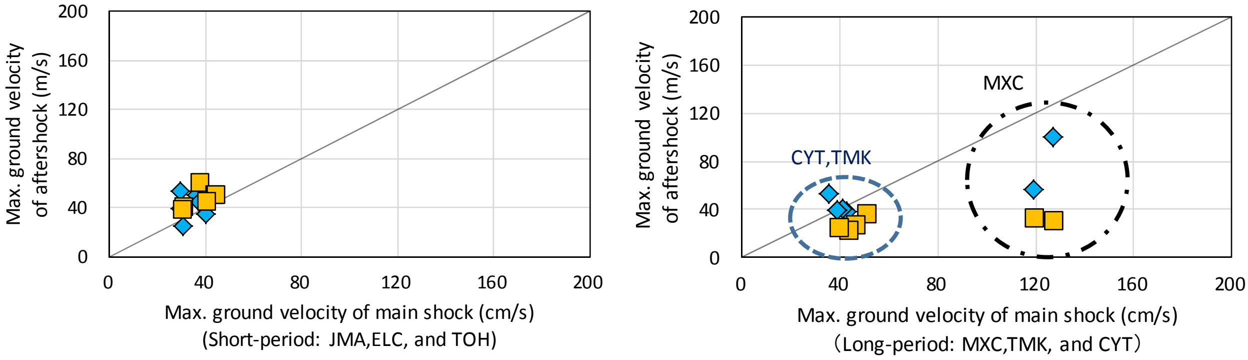

(b) Model S2

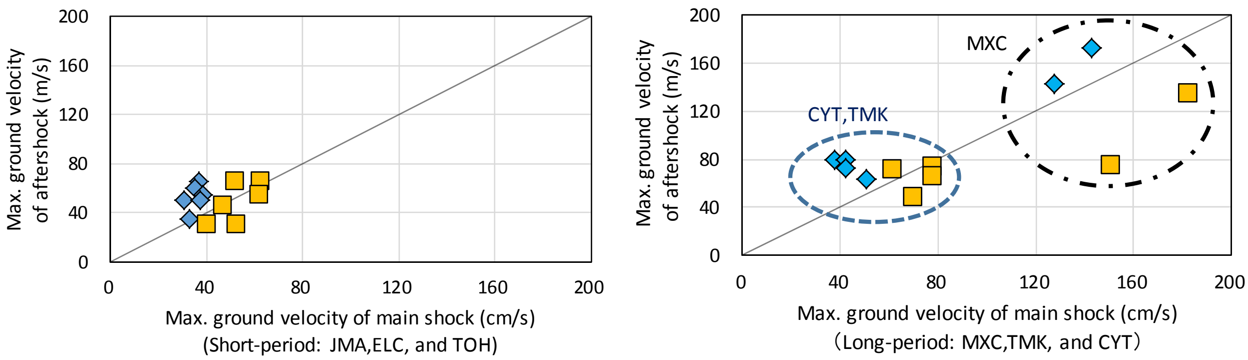

(c) Model FS1

Fig. 8 – Comparison of ground-motion levels (main shock versus aftershock)

Note that the elongation of the natural period increases as the strength deterioration after maximum load increases for the same drift level in the main shock due to the large deterioration of equivalent stiffness, as shown in Fig. 9, which compares the two cases. Thus, in Fig. 8, the maximum ground velocities in the aftershock for column S2 are smaller than those for column FS1 for long-period ground motions, even though they have the same collapse drift, because the buildings with long equivalent periods (S2 > FS1) resonate more easily with long-period input motions.

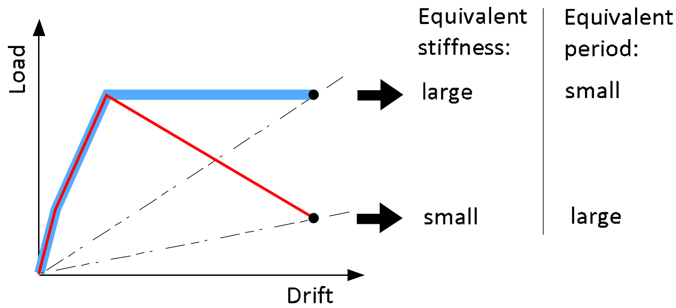

Fig. 9 – Comparison of framework of column

3.3 Comparison of ground-motion levels of the aftershock that induce collapse

The Relation between the maximum drift level in the main shock and the level of the aftershock that induces collapse is discussed. In this section, analytical results for nine-story buildings are stated. Fig. 10 shows the maximum drift level in the main shock versus the maximum ground velocity of the aftershock that induces collapse relations for three cases: (a) column S1; (b); column S2; and (c); column FS1. Fig. 10 also shows average values of the maximum ground velocity in the aftershock for short- and long-period ground motions.

According to Fig. 10(a) and (b), for columns S1 and S2, the average value of short-period ground motions increases with the increase of the maximum drift level in the main shock. This result indicates that the smaller the maximum drift in the main shock, the smaller the ground motion level of the aftershock that induces collapse for short-period ground motions. This is different from the general perception. This finding shows, as stated above, that elongation of the period of buildings due to the large plastic response in the main shock induces the discrepancy between the period of buildings and the period of ground motions of short-period aftershocks. Fig. 11 shows S1column damage with maximum drifts of 2.7% (30% of collapse drift) and 8.0% (90% of collapse drift) in the main shock. Fig. 11 also shows the maximum ground velocities of the aftershock that induces collapse for the two cases for earthquake JMA. For the maximum drift in the main shock of 30% of the collapse drift, the column damage is rather small, whereas the maximum ground velocity of the aftershock that induces collapse is smaller than that of the maximum drift in the main shock of 90% of the collapse drift, where remarkable damage occurs. This result indicates that if a building damaged after the main shock experiences only small drifts and seems to have slight damage, it can collapse from a smaller aftershock.

According to Fig. 10(b) and (c), the average values of long-period ground motions decrease with the increase in the maximum drift in the main shock, contrary to those of short-period ground motions. This finding shows, as stated above, that elongation of the period of buildings in the main shock induced consistency between the period of buildings and that of ground motions of long-period aftershocks.

According to Fig. 10(a) and (b), the maximum ground velocities that induced collapse as a result of aftershocks for column S2 are smaller than those for column S1. This is because column S2 has smaller collapse drift than column S1. According to Fig. 10(b) and (c), the maximum ground velocities of column S2 are smaller than those of column FS1, although the two models have the same collapse drift. This is because the column S2 has larger load-degrading after maximum load than column FS1.

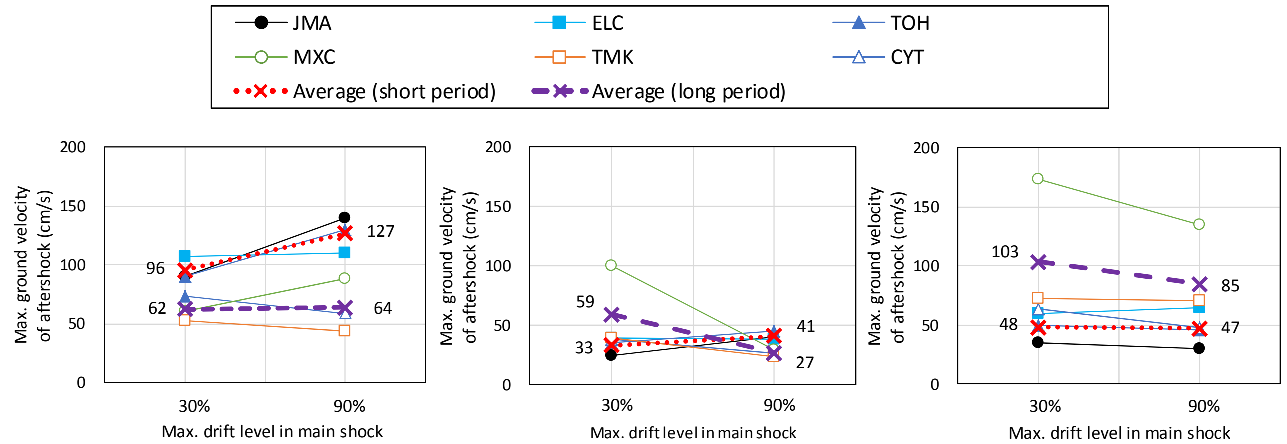

(a) Column S1 (b) Column S2 (c) Column FS1

Fig. 10 – Maximum drift level in main shock versus maximum ground velocity of aftershock that induces collapse (nine-story building)

Damage condition		
Max. drift in main shock	2.7% (30% of collapse drift)	8.0% (90% of collapse drift)
Max. ground velocity of aftershock that induces collapse	90 cm/s	140 cm/s

Fig. 11 – Damage condition, maximum drift in main shock, and maximum ground velocity of aftershock that induces collapse (nine-story building, column S1, and JMA)

3.4 Effect of number of stories

To examine the effect of the number of stories on collapse, the ground motion levels (maximum ground velocity) of aftershocks for the number of stories are compared. Fig. 12 shows the number of stories versus maximum ground velocity of the aftershock that induces collapse relations for three cases: (a) column S1; (b); column S2; and (c); column FS1. The maximum drift in the main shock is 30% of the collapse drift. Fig. 12 also shows average values of the maximum ground velocity for short- and long-period ground motions, respectively. According to Fig. 12, the average values decrease with an increase in the number of stories irrespective of the predominant periods (short period or long period) of ground motions. In other words, the more stories a building has, the smaller the ground motion level of the aftershock that induces collapse. The reason for this can be described as follows: Once a collapse story suffers heavy damage, lateral drifts of other stories decrease and concentrate on the collapse story. In other words, the more stories a building has, the larger the maximum drift of the collapse story. This result indicates that high-rise buildings are more likely to suffer intermediate-story collapse than low-rise buildings, and that the former are more dangerous than the latter, even when the buildings have the same I_S value (i.e., the buildings are judged to have the same seismic performance based on Japanese seismic evaluation).

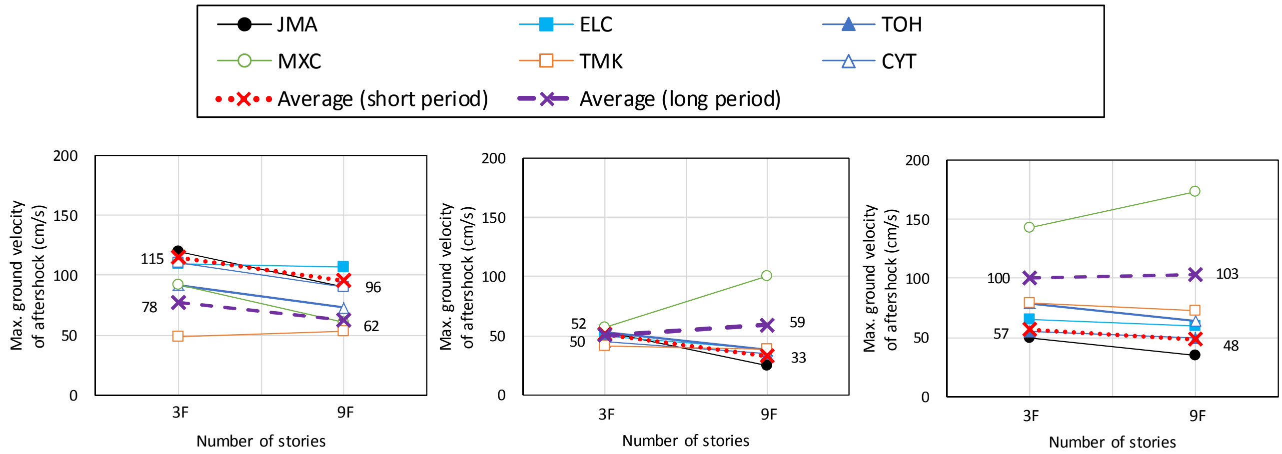

(a) Column S1 (b) Column S2 (c) Column FS1

Fig. 12 – Number of stories versus maximum ground velocity of aftershock that induces collapse (maximum drift in main shock = 30% of collapse drift)

4. Conclusions

The dynamic responses and intermediate-story collapse behavior of RC buildings based on the pre-1971 building code are studied. The effect of aftershocks after the main shock is evaluated. The major findings from this study are as follows:

(1) For short-period ground motions, the smaller the maximum drift in the main shock, the smaller the ground motion level of the aftershock that induces collapse. This finding shows that elongation of the period of buildings due to the large plastic response in the main shock induces discrepancy between the period of buildings and that of short-period ground motions of aftershocks. Thus, if a building damaged after the main shock experiences only small drifts and seems to have slight damage, it can collapse from a smaller aftershock when the ground motion has a short-period element.

(2) For long-period ground motions, the ground-motion level of the aftershock that induces collapse is smaller than that for short-period ground motions even when buildings suffer the same maximum drift in the main shock. This result indicates that if a building with large collapse drifts experiences large response drifts and suffers severe damage from the main shock, long-period ground motions are more dangerous for the building than short-period ground motions.

(3) The maximum ground velocity that induces collapse as a result of aftershocks decreases as the collapse drift decreases, and load-degrading decreases even if the maximum drift in the main shock remains constant.

(4) The more stories a building has, the smaller the ground motion level of the aftershock that induces collapse. Thus, high-rise buildings are more likely to suffer intermediate-story collapse, and are therefore more dangerous than low-rise buildings, even when the buildings are judged to have the same seismic performance.

Acknowledgements

This study was supported by the Japan Society for the Promotion of Science Grants-in-Aid for Scientific Research Grant: Number 25420573.

Appendix

The seismic capacity index I_S is given as follows [5, 6]:

$$I_S = E_0 \cdot S_D \cdot T\,, \tag{1}$$

where S_D is the configuration index (assumed to be 1.0 for this study), T is the time index, (assumed to be 1.0 for this study), and E_0 is determined as follows:

$$E_0 = (1 / A_i) \cdot C \cdot F\,, \tag{2}$$

where A_i is the vertical distribution factor of story shear coefficients in Japanese building codes, and i is the story to be studied. The index C is defined as the strength of a column divided by the total weight of the floors above the column, whereas the index F is determined according to the deformability of the column. For the columns in this study, F was calculated to be 1.0.

References

[1] Raghunandan M, Liel A B, Ryu H, et al. (2012): Aftershock Fragility Curves and Tagging Assessments for a Mainshock-Damaged Building, Proceedings of the fifteenth World Conference in Earthquake Engineering

[2] Jeon J S, DesRoches R, Brilakis I, Lowes L N (2012): Aftershock Fragility Curves for Damaged Non-Ductile Reinforced Concrete Buildings, Proceedings of the fifteenth World Conference in Earthquake Engineering

[3] Figueroa M. Diaz, Koichi Kusunoki, Akira Tasai (2013): Analytical Study on the Seismic Performance Estimation using the Equivalent Damping and Response Reduction Ratio for Aftershocks, Journal of Structural Engineering, AIJ and JSCE, Vol.59B, pp.399-408

[4] Takaine Y, Nakamura T and Yoshimura M (2003): *Collapse Drift of Reinforced Concrete Columns*, Journal of Structural and Construction Engineering, Architectural Institute of Japan, No. 573, pp. 153-160 (in Japanese).

[5] Japan Association for Building Disaster Prevention (2001): *Standard for Seismic Evaluation of Existing RC Buildings* (in Japanese)

[6] Otani S (2003): *Seismic Vulnerability Assessment and Retrofit - State of Practice in Japan* -, Proceedings of the fib 2003 Symposium - Concrete Structures in Seismic Regions -, pp. 43-62.

[7] Tamura M and Tanaka A (1999): *Statistical Study on the Evaluation of Seismic Capacity of Existing RC Buildings*, Journal of Structural Engineering, Architectural Institute of Japan, Vol. 45B, pp. 297-304 (in Japanese).

[8] Eto H and Takeda T (1977): *Inelastic Earthquake Response Frame Analysis of Reinforced Concrete Structures*, Summaries of Technical Papers of Annual Meeting, Architectural Institute of Japan, pp.1877-1878 (in Japanese).

[9] Newmark N M (1959): *A Method of Computation for Structural Dynamics*, Proc. ASCE, Vol.85, EM3, pp.67-94

[10] Evaluation Committee of High-rise Buildings (1986): *Seismic Ground Motion for Dynamic Analysis of High-rise Buildings*, The Building Center of Japan, Building Letter for June, pp.49-50 (in Japanese)